International Journal of Mass Spectrometry 390 (2015) 170–177

Contents lists available at ScienceDirect

International Journal of Mass Spectrometry

journal homepage: www.elsevier.com/locate/ijms

Dissociation of proton-bound complexes reveals geometry and arrangement of double bonds in unsaturated lipids

Huong T. Pham[a], Matthew B. Prendergast[b], Christopher W. Dunstan[b], Adam J. Trevitt[b,e], Todd W. Mitchell[d], Ryan R. Julian[a,*], Stephen J. Blanksby[b,c,e,**]

[a] Department of Chemistry, University of California, Riverside, USA
[b] School of Chemistry, University of Wollongong, Australia
[c] Central Analytical Research Facility, Queensland University of Technology, Australia
[d] School of Medicine, University of Wollongong, Australia
[e] ARC Centre of Excellence for Free Radical Chemistry and Biotechnology, Australia

ARTICLE INFO

Article history:
Received 2 May 2015
Received in revised form 13 July 2015
Accepted 15 July 2015
Available online 23 July 2015

Keywords:
Lipids
Isomers
Non-covalent complex
Collision-induced dissociation
Radicals
Carbenes

ABSTRACT

Double bond position and stereochemistry in unsaturated lipids can have profound impact on biological properties and activities but the assignment of these features by mass spectrometry is frequently challenging. Conventional techniques for lipid identification rely on collision-induced dissociation (CID) and are most often unable to differentiate between lipid isomers, particularly those involving double bond position and geometry (*i.e.*, *cis* and *trans*). In this study, CID performed on proton-bound complexes of fatty acid methyl esters and iodoaniline (and related reagents) reveals unusual fragmentation patterns. CID products are shown to result from proton transfer and are associated with specific structures of the unsaturated lipids. Notably, CID of these complexes can not only distinguish *cis*- and *trans*-fatty acid methyl esters, but also differentiate *conjugated* double bond arrangements from *non-conjugated* analogs. Herein, the mechanisms underpinning this unique CID behavior are investigated by stable isotope labeling and are proposed to involve both carbene and free radical intermediates.

1. Introduction

Double bond stereochemistry and positional arrangement in unsaturated lipids can have profound impact on biological properties and activities [1–3]. However, determination of these critical features by mass spectrometry is challenging. Conventional low energy collision-induced dissociation (CID) is the mainstay of modern lipid analysis but for isomeric lipids CID mass spectra are often similar or identical, particularly where isomers differ only in double bond position and geometry (*i.e.*, *cis* and *trans* isomers) [4]. As a result, many studies have attempted to enhance CID with either chemical derivatization of carbon-carbon double bonds or the introduction of targeted radical dissociation processes in order to obtain greater structural information. One example of the former is to convert olefinic bonds to secondary ozonides, which can then undergo ionization in either positive or negative ion mode electrospray ionization (ESI). Subsequent CID yields diagnostic products that allow the determination of double bond position(s) [5,6]. In the same manner, Moe et al. pre-treated phospholipids and free fatty acids with osmium tetroxide (OsO_4) prior to electrospray ionization. This method derivatized double bonds to vicinal diols, which are readily cleaved upon CID, enabling identification of initial double bond location [7]. Another method employs ion-molecule reactions between unsaturated lipids and ozone in the gas phase, namely ozone-induced dissociation (OzID) for *online* assignment of the double bond position(s) [8,9]. Moreover, the differences in reaction rates for gas-phase ozonolysis (and thus product ion abundance) have been exploited to discriminate between lipid geometric isomers (*i.e.*, *cis* and *trans* isomers) [10]. Dramatic differences in gas phase reaction rates have also been noted between *conjugated* and *non-conjugated* linoleic acid methyl esters [11]. Although capable of detecting subtle structural differences, OzID technology is currently not widely available.

Radical-based dissociation techniques (*e.g.*, EID, ETD, ECD and RDD) have been applied to lipid analysis with the aim to induce carbon-carbon bond cleavages and thus to reveal more of the intra-chain bonding motifs (*i.e.*, double bond position, chain branching,

* Corresponding author at: Department of Chemistry, University of California, Riverside, USA. Tel.: +1 951 827 3958.
** Corresponding author at: Central Analytical Research Facility, Queensland University of Technology, Australia. Tel.: +61 731383343.
E-mail addresses: ryan.julian@ucr.edu (R.R. Julian), stephen.blanksby@qut.edu.au (S.J. Blanksby).

http://dx.doi.org/10.1016/j.ijms.2015.07.006
1387-3806/

etc.). For example, Yoo and Håkansson generated radical precursor ions at ~10 eV electron energy and performed electron-induced dissociation (EID) on unsaturated fatty acids with Mn^{2+} attached at the carboxylic acid moiety. The resulting fragmentation produced patterns associated with the double bond positions within the acyl chain [12]. Electron-capture dissociation (ECD) and electron-transfer dissociation (ETD) have also been applied to lipid structural analysis but in general do not yield greater insight than conventional CID [13,14]. Specifically, ECD and ETD examination of phospholipids yielded product ions identifying the lipid headgroup and the chain length and degree of unsaturation of the acyl chains but did not reveal information that is specific to the site of unsaturation nor stereochemistry of the double bond(s).

We have previously demonstrated another radical approach, namely radical directed dissociation (RDD), to be a sensitive structural tool for both proteins [15,16] and lipids [17–20]. In the RDD approach, bifunctional molecules containing a photo-activated radical initiator are adducted (either covalently or non-covalently) to a lipid, ionized and then subjected to laser irradiation in an ion-trap mass spectrometer. Subsequent, collisional activation of the resulting radicals yields rich and structurally informative fragmentation, especially for elucidating carbon-bonding motifs within lipid acyl chain substituents. For example, RDD was shown to discriminate between branched and straight-chain phospholipid isomers, and was effectively deployed to assign carbon-carbon double bond position(s) in unsaturated triacylglycerols [17]. Interestingly however, once the radical has been introduced into the carbon chain, it can scramble the geometry of the unsaturated center, making it insensitive for distinguishing *cis* and *trans* structures [18]. Serendipitously however, CID of some of the same non-covalent complexes between lipids with iodo-containing reagents—which had been initially designed for RDD—are found to undergo surprising even-electron fragmentation that is strongly associated with the geometry of the carbon-carbon double bond. This observation is described herein for fatty acid methyl ester (FAME) lipids with *cis/trans* and *conjugated/non-conjugated* structures. The fragmentation mechanism is investigated by stable isotope labeling experiments and provides further understanding that may support future applications of this approach to the field of lipidomics.

2. Experimental methods

2.1. Materials

The following fatty acid standards: oleic acid FA 18:1(9*Z*), elaidic acid FA 18:1(9*E*), *cis*-vaccenic acid FA 18:1(11*Z*), *trans*-vaccenic acid FA 18:1(11*E*), palmitoleic acid FA 16:1(9*Z*), palmitelaidic acid FA 16:1(9*E*) were purchased from Nu-Chek Prep (Elysian, Minnesota) and were all ~99% purity. Three linoleic acid methyl ester isomers, FAME 18:2(9*Z*,12*Z*), FAME 18:2(10*E*,12*Z*) and FAME 18:2(9*Z*,11*E*), were also purchased from Nu-Chek Prep (Elysian, Minnesota). D_{17}-Oleic acid (containing 17 deuterium atoms at the 11, 11′, 12, 12′, 13, 13′, 14, 14′, 15, 15′, 16, 16′, 17, 17′, 18, 18′, and 18″ positions, ~99% deuterium incorporation) was obtained from Cayman Chemical (Ann Arbor, MI).

Boron trifluoride-methanol 10% solution, D_1-methanol (CH_3OD), D_3-methanol (CD_3OH), deuterium oxide (D_2O) and all iodo-containing reagents: 2-iodoaniline (*o*IA), 3-iodoaniline (*m*IA), 4-iodoaniline (*p*IA), 4-iodobenzylamine (IBzA) and 3-iodo-4-methylaniline (IMeA) were obtained from Sigma–Aldrich (St. Louis, MO). Other HPLC grade solvents, such as methanol, chloroform and *n*-pentane, were purchased from Thermo-Fisher Scientific (Waltham, MA) and were used without further purification.

2.2. Sample preparation

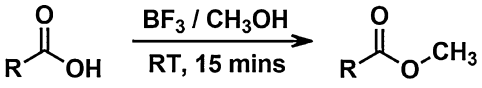

(1)

The procedure to convert fatty acids (FA) to fatty acid methyl esters (FAME) was described previously and is summarized in Eq. (1) [20]. Briefly, the FA (~1 mg) was treated with BF_3 in a 10% methanol solution at room temperature (RT) and then extracted into a non-polar solvent (*e.g.*, *n*-pentane). Fresh samples were prepared for mass spectrometry by collecting the upper *n*-pentane layer (~3 mM) and diluting in methanol to yield of final solution of 10–20 μM in the resulting FAME. Then, each iodine-containing reagent was added to a sample of this solution to a final concentration of 5–10 μM before adding 0.05% formic acid to aid the formation of protonated 4-iodoaniline (*p*IA) for charge adducting.

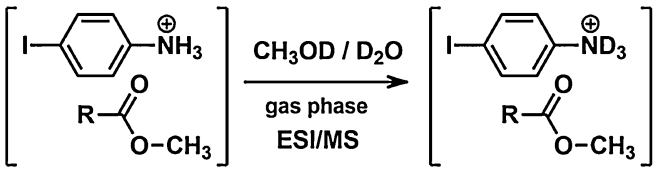

(2)

Deuterium-exchanged experiments were undertaken as summarized in Eq. (2), whereby a mixture of D_1-methanol and D_2O (2:1) was used to dilute 1 μL of the *n*-pentane layer to exchange all three protons in protonated amine group ($-ND_3^+$).

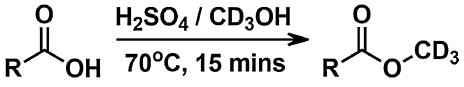

(3)

Preparation of the D_3-labeled FAME 1,1,1-trideuteromethyl (*Z*)-octadec-9-enoate is summarized in Eq. (3). In this procedure, 9*Z*-ocatadecanoic acid (1 mg, 4 μmol) placed in D_3-methanol (CD_3OH, 100 μL), with the addition of sulfuric acid (2%), was heated at 70 °C for 15 min in an oil bath and then allowed to cool for 15 min. Milli-Q water (1 mL) and *n*-pentane (1 mL) were added to the solution. After vigorous shaking, to ensure thorough mixing, the mixture was left for 30 min at 4 °C to allow the separation of the aqueous and organic layers. The *n*-pentane layer was collected with a Pasteur pipette and was prepared for mass spectrometric analysis as described above.

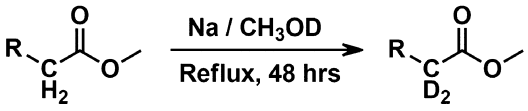

(4)

Methyl (*Z*)-2,2-dideutero-octadec-9-enoate was prepared by adapting a procedure previously used to synthesize methyl 2,2-dideuteropentanoate and is summarized in Eq. (4) [21]. D_1-Methanol (CH_3OD, 8.13 g, 246 mmol) was cooled in an ice-bath under a nitrogen atmosphere and sodium metal (75.4 mg, 3.28 mmol) was added. After the metal had dissolved, 3.25 mL of the solution was added to methyl (*Z*)-octadec-9-enoate (1.00 g, 3.71 mmol) and the resulting mixture heated at reflux under nitrogen for 48 h. The solvent was removed *in vacuo* to yield the product as brown oil. The sample was then prepared for mass spectrometric analysis as described above.

2.3. Mass spectrometry

Experiments were performed using a linear ion-trap mass spectrometer, Thermo Fisher Scientific LTQ (San Jose, California). Sample solutions were introduced into the electrospray ionization

by direct infusion to generate the gaseous non-covalent complexes. Typical source parameters included: spray voltage +4.0–4.5 kV; capillary temperature 250 °C, capillary voltage 5–11 V, and tube lens voltage 25–40 V. Nitrogen served as sheath, sweep and auxiliary gases and all were set to between 5 and 20 (arbitrary units) and helium was used as buffer/collision gas. Ions were mass-selected with an isolation width of 1–3 Da and activated by collision-induced dissociation (CID) using default instrument MS^n parameters. Mass spectra were typically averaged over 50–100 scans to obtain the desired signal-to-noise.

3. Results and discussions

3.1. *Differentiation of* cis *and* trans *isomers*

Neutral glycerolipids readily form non-covalent complexes with ammonium ions and CID of the resulting complexes is widely used for structural analysis [22]. Such complexation is similarly efficient for aniline-derived compounds [17,18]. Fig. 1(a-e) shows the CID spectra obtained for complexes of FAME 18:1(9*Z*) with (a) 4-iodobenzylamine and (b-e) four different iodo-aniline variants. The most abundant product ion in each case corresponds to the ammonium cation (specific structures shown in red) occurring at either *m/z* 234 or *m/z* 220, depending on the mass of the adducting amine. These ions are formed by simple dissociation of the non-covalent bond and neutral loss of the lipid. Fig. 1(a) shows an additional product ion at *m/z* 217, which is a secondary loss of ammonia (−17 Da) originating from iodobenzyl ammonium cation at *m/z* 234.

In addition to the abundant ammonium ions observed in all spectra shown in Fig. 1, for the *m*IA and *p*IA complexes (Fig. 1d and e, respectively) there are also two interesting product ions of appreciable abundance at *m/z* 297 and *m/z* 295. Of these peaks, only the *m/z* 297 peak is observed for *m*IA (Fig. 1d), while both *m/z* 295 and 297 are of comparable abundance for the *p*IA (Fig. 1e). Neither of these product ions are observed for the IBzA complex (Fig. 1a), and they are only present at very low abundance for the IMeA and *o*IA complexes (Fig. 1b and c, respectively). Focusing on the *p*IA complexing reagent which produces both the *m/z* 295 and 297 ions, the ratio of these two peaks was found to invert if the stereochemistry of the double bond is *cis* or *trans* as illustrated with the FAME 18:1(9*E*) isomer in Fig. 1(f). Therefore, the products at *m/z* 295 and 297 are sensitive to both the structure of the complexation reagent

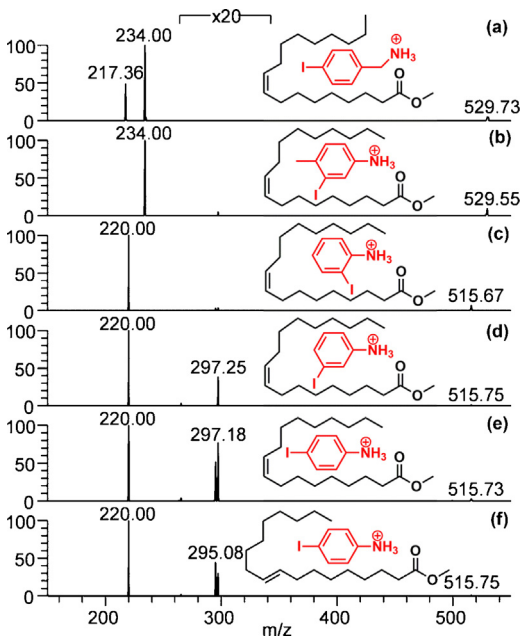

Fig. 1. CID of non-covalent complexes between (a-e) oleic acid methyl ester FAME 18:1(9*Z*) and five different iodine-containing reagents with structures noted in red (f) elaidic acid methyl ester FAME 18:1(9*E*) and *p*IA. The 20× magnification indicated at the top is applied to all spectra.

and, in the case of the *para*-iodoaniline variant, to the stereochemistry of the double bond. Substitution of bromo- for iodo-aniline within the proton-bound complex results in loss of the *m/z* 295 feature for all isomers (one such example is shown in Supporting Information, Figure S-1). Furthermore, these product ions are not observed if the complex is subjected to UV irradiation, which primarily results in homolytic cleavage of the carbon-iodine bond and subsequent radical directed dissociation products.

To examine the generality of these observations, several additional lipids were examined with the *p*IA reagent. Fig. 2 shows the CID mass spectra for two pairs of geometrical isomers, namely FAME 18:1(11*Z*) and FAME 18:1(11*E*) (Fig. 2a and b, respectively) and FAME 16:1(9*Z*) and FAME 16:1(9*E*) (Fig. 2c and d, respectively). Again the ratio of the product ion abundances of *m/z* 297 and *m/z* 295 for the 18:1 isomers and the equivalent *m/z* 269 and

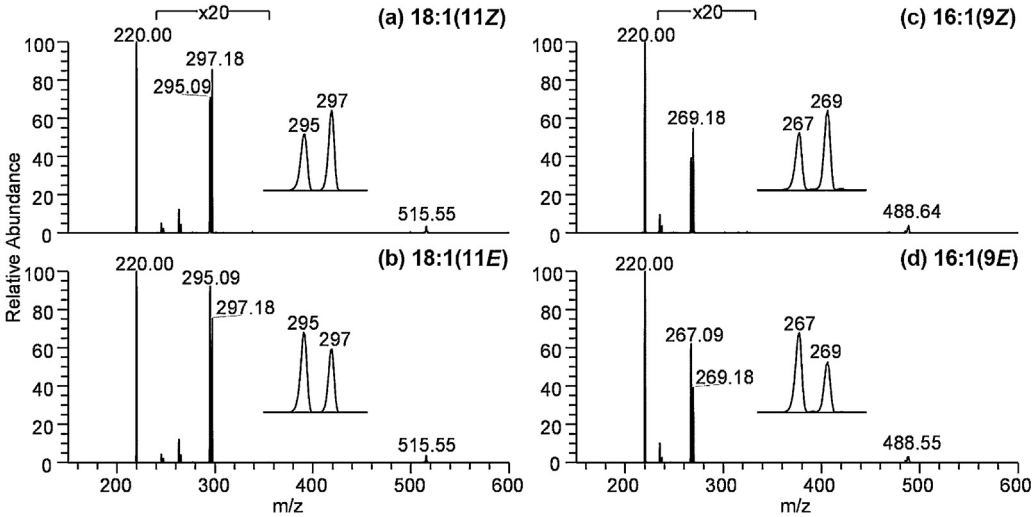

Fig. 2. CID of non-covalent complexes of [FAME + *p*IA]$^+$ precursor ion from two pairs of stereoisomers (a) FAME 18:1(11*Z*), (b) FAME 18:1(11*E*), (c) FAME 16:1(9*Z*) and (d) FAME 16:1(9*E*).

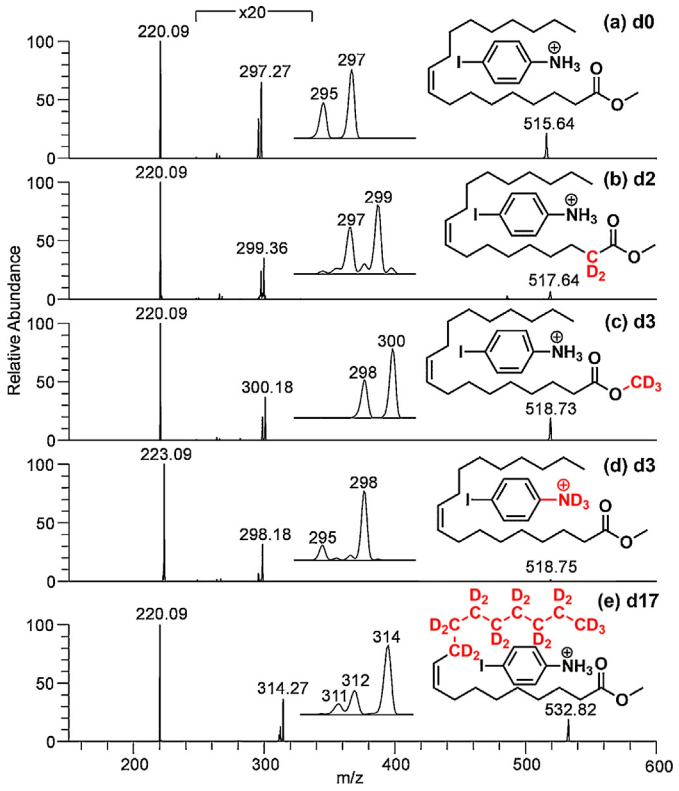

Fig. 3. CID spectra acquired for (a) the unlabeled standard [FAME 18:1(9*Z*) + *p*IA]$^+$ at *m/z* 516, (b) the D_2-labeled [D_2-FAME 18:1(9*Z*) + *p*IA]$^+$ at *m/z* 518, (c) the D_3-labeled [D_3-FAME 18:1(9*Z*) + *p*IA]$^+$ at *m/z* 519, (d) the D_3-exchanged complexes [FAME 18:1(9*Z*) + D_3-*p*IA]$^+$ at *m/z* 519 and (e) the D_{17}-labeled lipid standard [D_{17}-FAME 18:1(9*Z*)-d17 + *p*IA]$^+$ at *m/z* 533. Deuterium incorporation is illustrated in Supporting Information (Figure-S2).

m/z 267 ion pair for the 16:1 isomers are shown to be sensitive to the stereochemistry of the carbon-carbon double bond. Furthermore, these data demonstrate that the dissociation pathway yielding these fragments can occur at different double bond locations (*i.e.*, 9- and 11-positions) and with varying chain lengths (*i.e.*, 16- and 18-carbon variants).

3.2. Deuterium labeling

In order to probe the mechanisms yielding the diagnostic products ions identified above, a series of deuterium-labeling experiments were carried out and the results are summarized in Fig. 3. Where the lipid carries the deuterium label, direct dissociation of the complex yields unlabeled anilinium ions at *m/z* 220 (see Fig. 3b, c and e) while exchange of the anilinium protons for deuterium results in a quantitative shift of this ion to *m/z* 223 (Fig. 3d). These observations suggest that there is no hydrogen scrambling within the complex prior to dissociation. The 2 Da spacing between fragments of interest observed at *m/z* 295 and 297 for the unlabeled archetype (Fig. 3a) is conserved when the lipid is deuterium labeled at the labile α-carbon (Fig. 3b) or the ester methyl group (Fig. 3c). This suggests that neither site plays a significant mechanistic role in the fragmentation processes. Exchange of the anilinium protons (Fig. 3d) increases the spacing between the ions of interest to 3 Da. Importantly, the peak observed at *m/z* 298 results from transfer of a deuteron to the lipid, increasing the mass by 1 Da while the peak at *m/z* 295 is not shifted, suggesting no transfer of a deuteron or scrambling with the lipid occurs in the formation of this ion. In Fig. 3(e), labeling of the final 17-positions of the lipid alkyl chain is shown to produce loss of both two hydrogen atoms yielding a product ion at *m/z* 312 and one hydrogen and one deuterium atom to yield *m/z* 311 with the former process being favored. The data in Fig. 3(e) suggest that hydrogens from either half of the lipid can be lost in formation of the marker ion at *m/z* 295. Given the previously demonstrated stereochemical sensitivity of this pathway, the most likely positions are the two sites allylic to the carbon-carbon double bond.

Based on the results presented in Figs. 1–3, we propose the mechanism shown in Scheme 1 to explain the diagnostic product ions at *m/z* 295 and 297. As the first step toward formation of the product at *m/z* 295, a proton is transferred from the amine to the *ortho*-position on the aniline ring. The energetics of the ring-protonated tautomers of the anilinium cation have previously been calculated, and the *ortho*-site is found to have a proton affinity only 11 kJ mol^{-1} lower than the nitrogen while the *para*-site is slightly *favored* over nitrogen for protonation by 8 kJ mol^{-1} [23]. While the effect of iodine on the relative energetics of these tautomers has not been reported, it is reasonable to suppose that protonation of the *ortho*-, *meta*- and *para*-positions of iodoanilines is similarly thermoneutral. While protonation of the ring is energetically reasonable, barriers to intra-molecular proton transfer have been calculated to be substantial, *e.g.*, proton transfer from nitrogen to the *ortho*-carbon is calculated to be 238 kJ mol^{-1} for the anilinium cation. In this case however, the analogous proton migration can be catalyzed by the adducted lipid. The methyl ester moiety in particular could play a crucial role in shuttling the proton between the nitrogen and the ring and even between positions on the ring at relatively modest energetic cost [24]. Once the proton has migrated to the *para*-position, the activated system is configured for loss of hydrogen iodide producing a resonance-stabilized carbene and placing the formal charge back on the nitrogen. This intermediate carbene could insert into an allylic C—H bond on either side of the double bond, temporarily fusing the two molecules. At this point, the lipid-ring bond is cleaved in an electron transfer process driven by formation of aniline and the lipid is released as a carbocation at *m/z* 295. The *meta*-iodoaniline cannot form a resonance-stabilized carbene intermediate, which may explain the absence of a product ion at *m/z* 295 in Fig. 1(b) or (d). Although the *ortho*-iodoaniline could form a resonance-stabilized carbene, it is likely that proximity to the amine prevents loss of HI by facilitating the reverse proton transfer. The combination of these resonance and steric effects can account for the spectral differences between the *ortho*-, *meta*- and *para*-isomers observed in Fig. 1. Furthermore in this mechanism, a hydrogen is abstracted *from* the lipid without transfer of a proton *to* the lipid, which is consistent with the absence of deuterium scrambling observed in Fig. 3(d) and the loss of deuterium observed in Fig. 3(e). Finally, the insertion of the carbene into the allylic C—H bond is central to the proposed mechanism. The energetics of these bonds will be subtly different within the *cis* and *trans* isomers providing a rationale for the differing relative abundance of the *m/z* 295 and 297 signals for each of the lipids (see examples in Fig. 2). Collision energy was found to alter the abundance ratio of the *m/z* 295 and 297 product ions but the *m/z* 295 channel is consistently favored for the *trans* isomer while the *m/z* 297 channel is preferred for the *cis* isomer at all energies explored (Supporting Information, Figure S-5). The observed variation of the *m/z* 295 and 297 product ion abundances with collision energy (see breakdown curves shown in Supporting Information, Figure S-6) is consistent with the different kinetic constraints of the two competing processes shown in Scheme 1 (*i.e.*, proton transfer compared to rearrangement).

The ion at *m/z* 297 arises from simple proton transfer from the aniline to the lipid. The near exclusive transfer of a deuteron from D_3-iodoanilinium cation to the lipid (Fig. 3d) suggests that proton transfer from the ring protonated states does not occur to a significant extent. If this were the case, significant scrambling would be expected since the deuteron transfer to ring creates the potential for both deuteron and proton transfer. The overall low

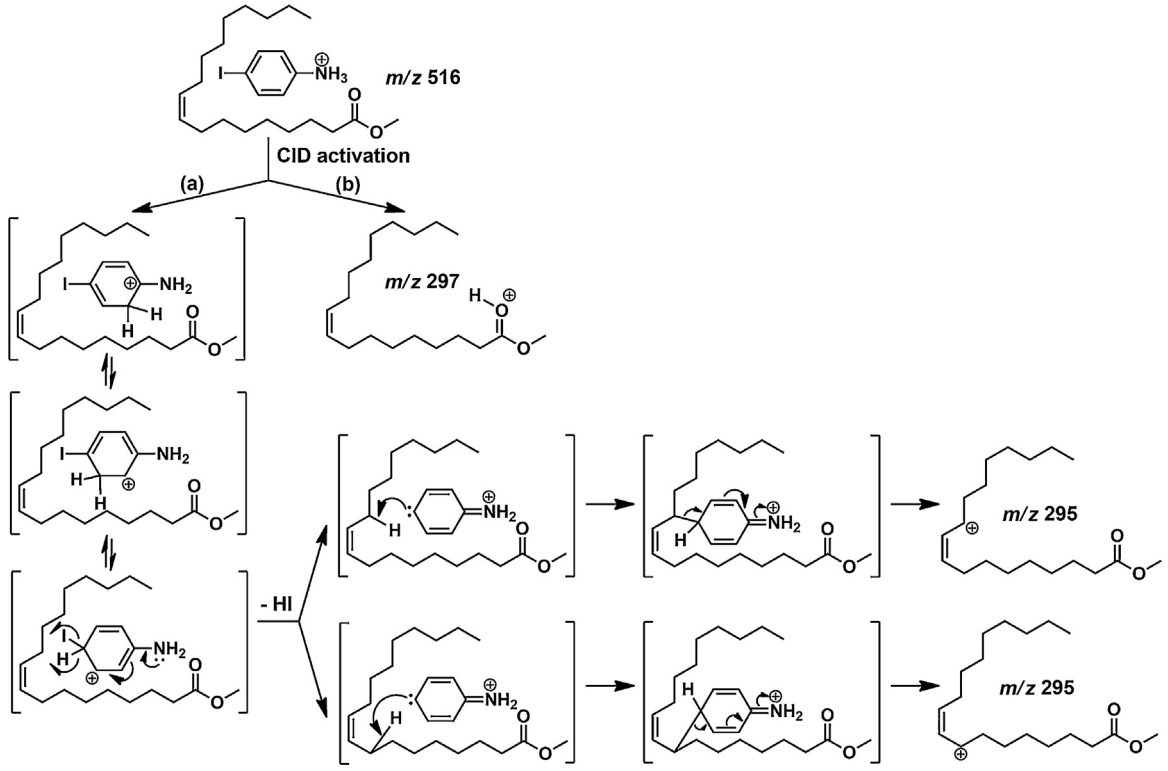

Scheme 1. Proposed mechanism for the formation of *m/z* 297 and 295 product ions shown in Fig. 3(a) from CID of the non-covalent complex [FAME 18:1(9*Z*) + *p*IA]$^+$ *m/z* 516 precursor ion.

abundance of the protonated lipid at *m/z* 297 compared to the anilinium and benzylammonium ions at *m/z* 220 and 234 (see Fig. 1) is consistent with the relative expected proton affinities of the lipid (*e.g.*, PA[$CH_3CO_2CH_3$] = 822 kJ mol^{-1}) and aniline (*e.g.*, PA[$C_6H_5NH_2$] = 883 kJ mol^{-1}) [25].

3.3. Conjugated/non-conjugated lipids

Lipids commonly carry multiple double bonds with the relative arrangement and stereochemistry of these motifs giving rise to many isomeric variants. Examination of the dissociation behavior of *p*IA complexes with polyunsaturated lipids containing both conjugated and non-conjugated double bonds are shown in Fig. 4.

As seen in Fig. 4(a), the CID fragmentation for non-conjugated FAME 18:2(9*Z*,12*Z*) is very similar to that observed for the mono-unsaturated cases previously discussed (see for example, Fig. 1e and f). This implies that non-conjugated double bonds react in the same fashion as single double bonds. The spectra in Fig. 4(b) and (c) are notably different from Fig. 4(a), revealing that conjugated isomers (9*Z*,11*E*) and (10*E*,12*Z*) exhibit behavior distinct from the non-conjugated variant. There are several new or significantly enhanced reaction channels for the conjugated isomers. Peaks at *m/z* 387, 263, and 245 represent new products. The peak at *m/z* 295 is analogous to the *m/z* 297 signal for the monounsaturated lipids discussed earlier but is much more abundant for the conjugated system, rivaling the abundance of the iodoanilinium cation at *m/z* 220. The fragments at *m/z* 263 and 245 are secondary products arising from the loss of methanol (−32 Da) and methanol/water (−50 Da) from the protonated lipid *m/z* 295. The relatively high abundance of *m/z* 295 ion in these spectra indicates a significantly higher proton-affinity of conjugated FAME compared to its non-conjugated isomer. Deuterium labeling indicates that the proton is derived from the anilinium nitrogen (see

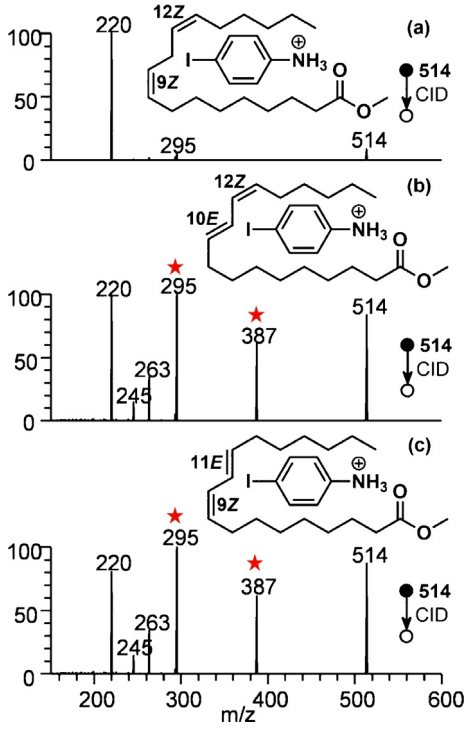

Fig. 4. CID spectra of non-covalent complexes [FAME + *p*IA]$^+$ from three isomers: (a) non-conjugated FAME 18:2(9*Z*,12*Z*), (b) conjugated FAME 18:2(10*E*,12*Z*) and (c) conjugated FAME 18:2(9*Z*,11*E*).

Supporting Information, Figure S-4) as previously observed for the mono-unsaturated lipids. The observation of greater abundance of the protonated FAME for the conjugated systems arises in part from the greater proton affinity of the conjugated double bonds

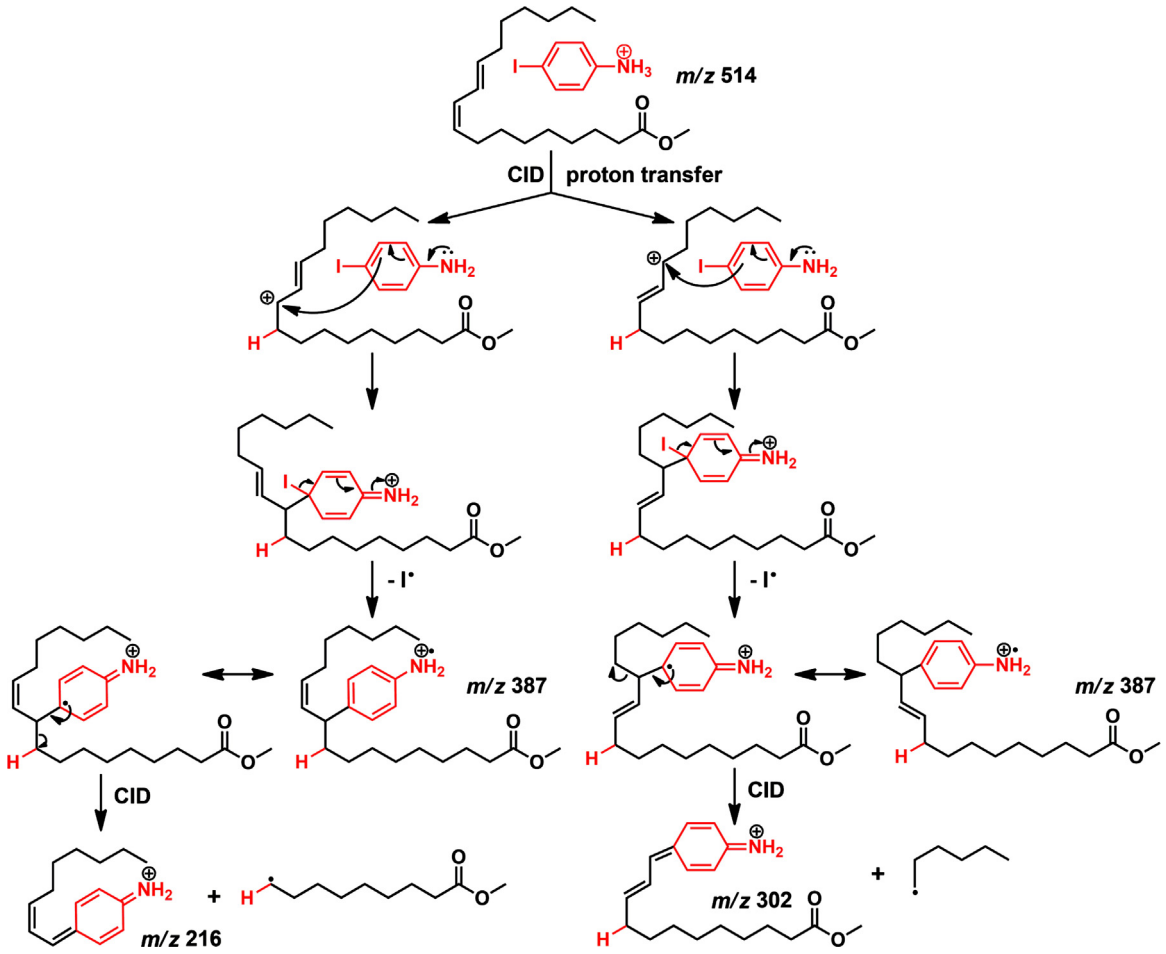

Scheme 2. Proposed mechanism with initial protonation of *conjugated* double bonds then inducing an electrophilic addition of the lipid to the aniline to form *m/z* 387 radical ion and two major MS^3 product ions at *m/z* 216 and 302 from [FAME 18:2(9*Z*,11*E*) + *p*IA]$^+$ in Fig. 5b.

themselves due to the potential for resonance stabilization of the resulting carbocation (*e.g.*, PA[2*E*-butene] = 747 kJ mol^{-1} compared to PA[1,3-butadiene] = 783 kJ mol^{-1}) [25]. When combined with additional stabilization afforded by interactions with the oxygens on the lipid ester moiety, the proton affinity appears to be nearly equal to that of *p*IA. Preference for proton transfer to the conjugated FAMEs interferes with the diagnostic dehydrogenation pathways that report on double bond geometry; however, the abundance of the proton transfer product itself clearly distinguishes the conjugated FAME from its non-conjugated isomers (Fig. 4).

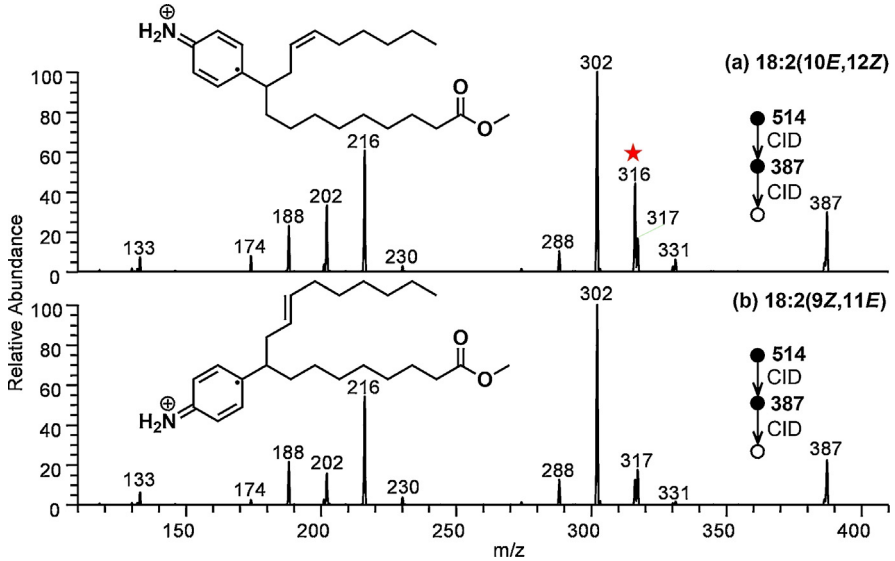

Fig. 5. MS^3 mass spectra performed on the radical product ions at *m/z* 387 generated in CID of the two non-covalent complexes between protonated *p*IA and *conjugated* isomers: (a) FAME 18:2(10*E*,12*Z*) and (b) FAME 18:2(9*Z*,11*E*).

The product ion observed at *m/z* 387 in Fig. 4(b) and (c) is generated by neutral loss of atomic iodine and is unique to the conjugated FAMEs. The observation of the *m/z* 387 ion in these spectra is unusual as low energy CID does not commonly give rise to radical ions, a phenomenon commonly referred to as the even-electron rule [26]. Interestingly, this feature is not observed for *m*IA as shown in Figure S-3 (Supporting Information). We propose the mechanism shown in Scheme 2 to account for these observations and suggest that the same facile transfer of the proton between the anilinium ion and the conjugated double bond motif, as described above, can facilitate an electrophilic addition of the lipid to the aniline. Addition of the intermediate carbocation at the *para*-position on the aromatic ring will lower the bond dissociation energy of C—I bond and thus result in the homolytic cleavage of this bond and loss of atomic iodine. The resonance stabilization of the intermediate carbocation and the resulting radical by the aniline nitrogen is critical to these processes and thus explains the absence of such pathways for *m*IA. Evidence for the proposed covalent addition of the aniline to the alkyl chain is provided by the MS^3 spectra obtained from the radical anions of *m/z* 387 (Fig. 5). These spectra reveal abundant product ions at *m/z* 216 and *m/z* 302 that are consistent with cleavage of the alkyl chain occurring at or near the site of the aniline attachment. Consistent with this explanation, the abundance of the product ions arising from the intermediate radical cations appear to be sensitive to the arrangement of double bonds in the parent lipid and thus the MS^3 spectra could be used to distinguish between conjugated lipid isomers.

4. Conclusions

The photodissociation of non-covalent complexes of iodoanilines with neutral lipids has previously been demonstrated as an analytically powerful approach to lipid structure elucidation. This RDD approach is particularly useful for the assignment of position(s) of carbon-carbon double bonds and chain branching motifs in lipids [17]. Here we have shown, for the first time, that CID of these same complexes can also give rise to diagnostic fragments that report on complementary structural features, the most important of which is the stereochemistry of the carbon-carbon double bonds. While these diagnostic CID product ions were not observed for all the unsaturated lipids investigated, the fact that they can be derived from the same non-covalent complex used for RDD suggests that in future workflows may be possible that switch rapidly between RDD and CID analysis to more fully describe the structure of unknown lipids. Importantly, the diagnostic trend in ion abundance ratios is preserved across a wide range of collision energies (Supporting Information Figure S-5) and is also observed on instruments of different geometries (Supporting Information Figure S-6).

The chemistries giving rise to the diagnostic CID product ions are proposed to involve carbene and free radical intermediates formed within the non-covalent complex (see Schemes 1 and 2). If found to be general, such process could be exploited for structure elucidation in other classes of compounds or indeed, to explore the bimolecular gas phase chemistries of reactive intermediates.

Acknowledgements

S.J.B., A.J.T. and T.W.M. are grateful to the Australian Research Council (DP150101715 and DP120102922) and the University of Wollongong for funding. T.W.M. is an Australian Research Council Future Fellow (FT110100249) and S.J.B. and A.J.T. are supported by the Australian Research Council's Centre of Excellence for Free Radical Chemistry and Biotechnology (CE0561607). R.R.J and H.T.P acknowledge funding from the National Science Foundation (CHE 1401737). The authors thank Hill Harman (UCR) for stimulating discussion.

Appendix A. Supplementary data

Supplementary data associated with this article can be found, in the online version, at http://dx.doi.org/10.1016/j.ijms.2015.07.006

References

[1] C.-h. Huang, H.-n. Lin, S. Li, G. Wang, Influence of the positions of cis double bonds in the sn-2-acyl chain of phosphatidylethanolamine on the Bilayer's melting behavior, J. Biol. Chem. 272 (35) (1997) 21917–22192.
[2] Y. Lin, E. Schuurbiers, S. Van der Veen, E.A.M. De Deckere, Conjugated linoleic acid isomers have differential effects on triglyceride secretion in Hep G2 cells, Biochim. Biophys. Acta - Mol Cell Biol Lipids 1533 (1) (2001) 38–46.
[3] H.J. Heipieper, F. Meinhardt, A. Segura, The cis-trans isomerase of unsaturated fatty acids in Pseudomonas and Vibrio: biochemistry, molecular biology and physiological function of a unique stress adaptive mechanism, FEMS Microbiol. Lett. 229 (1) (2003) 1–7.
[4] S.J. Blanksby, T.W. Mitchell, Advances in mass spectrometry for lipidomics, Annu. Rev. Anal. Chem. 3 (1) (2010) 433–465.
[5] K.A. Harrison, R.C. Murphy, Direct mass spectrometric analysis of ozonides: application to unsaturated glycerophosphocholine lipids, Anal. Chem. 68 (1996) 3224–3230.
[6] S.R. Ellis, J.R. Hughes, T.W. Mitchell, M.i.h. Panhuis, S.J. Blanksby, Using ambient ozone for assignment of double bond position in unsaturated lipids, Analyst 137 (5) (2012) 1100–1110.
[7] M.K. Moe, T. Anderssen, M.B. Strom, E. Jensen, Total structure characterization of unsaturated acidic phospholipids provided by vicinal di-hydroxylation of fatty acid double bonds and negative electrospray ionization mass spectrometry, J. Am. Soc. Mass Spectrom. 16 (2005) 46–59.
[8] M.C. Thomas, T.W. Mitchell, D.G. Harman, J.M. Deeley, J.R. Nealon, S.J. Blanksby, Ozone-induced dissociation elucidation of double bond position within mass-selected lipid ions, Anal. Chem. 80 (1) (2008) 303–311.
[9] T.W. Mitchell, H.T. Pham, M.C. Thomas, S.J. Blanksby, Identification of double bond position in lipids: from GC to OzID, J. Chromatogr. B 877 (26) (2009) 2722–2735.
[10] B.L.J. Poad, H.T. Pham, M.C. Thomas, J.R. Nealon, J.L. Campbell, T.W. Mitchell, S.J. Blanksby, Ozone-induced dissociation on a modified tandem linear ion-trap: observations of different reactivity for isomeric lipids, J. Am. Soc. Mass Spectrom. 21 (12) (2010) 1989–1999.
[11] H. Pham, A. Maccarone, J.L. Campbell, T. Mitchell, S. Blanksby, Ozone-induced dissociation of conjugated lipids reveals significant reaction rate enhancements and characteristic odd-electron product ions, J. Am. Soc. Mass Spectrom. 24 (2) (2013) 286–296.
[12] H.J. Yoo, K. Håkansson, Determination of double bond location in fatty acids by manganese adduction and electron induced dissociation, Anal. Chem. 82 (16) (2010) 6940–6946.
[13] P.F. James, M.A. Perugini, R.A.J. O'Hair, Electron capture dissociation of complexes of diacylglycerophosphocholine and divalent metal ions: competition between charge reduction and radical induced phospholipid fragmentation, J. Am. Soc. Mass Spectrom. 19 (7) (2008) 978–986.
[14] X. Liang, J. Liu, Y. LeBlanc, T. Covey, A. Ptak, J. Brenna, S. McLuckey, Electron transfer dissociation of doubly sodiated glycerophosphocholine lipids, J. Am. Soc. Mass Spectrom. 18 (10) (2007) 1783–1788.
[15] T. Ly, R.R. Julian, Residue-specific radical-directed dissociation of whole proteins in the gas phase, J. Am. Chem. Soc. 130 (1) (2008) 351–358.
[16] X. Zhang, R.R. Julian, Investigating the gas phase structure of KIX with radical directed dissociation and molecular dynamics: retention of the native structure, Int. J. Mass Spectrom. 308 (2–3) (2011) 225–231.
[17] H.T. Pham, T. Ly, A.J. Trevitt, T.W. Mitchell, S.J. Blanksby, Differentiation of complex lipid isomers by radical-directed dissociation mass spectrometry, Anal. Chem. 84 (17) (2012) 7525–7532.
[18] H.T. Pham, A.J. Trevitt, T.W. Mitchell, S.J. Blanksby, Rapid differentiation of isomeric lipids by photodissociation mass spectrometry of fatty acid derivatives, Rapid Commun. Mass Spectrom. 27 (7) (2013) 805–815.
[19] H.T. Pham, R.R. Julian, Mass shifting radical delivery with crown ether attachment for separation and analysis of phosphatidylethanolamine lipids, Anal. Chem. 86 (6) (2014) 3020–3027.
[20] H.T. Pham, R.R. Julian, Radical delivery and fragmentation for structural analysis of glycerophospholipids, Int. J. Mass Spectrom. 370 (2014) 58–65.
[21] R.D. Bowen, H.G.M. Edwards, D.W. Farwell, S.E. Morgan, Raman spectroscopy of n-pentyl methyl ether and deuterium labelled analogues, J. Raman Spectrosc. 41 (12) (2010) 1725–1734.
[22] A.M. McAnoy, C.C. Wu, R.C. Murphy, Direct qualitative analysis of triacylglycerols by electrospray mass spectrometry using a linear ion trap, J. Am. Soc. Mass Spectrom. 16 (9) (2005) 1498–1509.

[23] R. Flammang, N. Dechamps, L. Pascal, Y. Van Haverbeke, P. Gerbaux, P.C. Nam, M.T. Nguyen, Ring versus nitrogen protonation of anilines, Lett. Org. Chem. 1 (1) (2004) 23–30.
[24] A.J. Chalk, L. Radom, Proton-transport catalysis: a systematic study of the rearrangement of the isoformyl cation to the formyl cation, J. Am. Chem. Soc. 119 (32) (1997) 7573–7578.
[25] P.J. Linstrom, W.G. Mallard (Eds.), NIST Chemistry WebBook, NIST Standard Reference Database Number 69, National Institute of Standards and Technology, Gaithersburg, MD 20899, 2015 http://webbook.nist.gov/ (retrieved April 30, 2015).
[26] K. Miriam, A. Mandelbaum, The 'even-electron rule', Org. Mass Spectrom. 15 (2) (1980) 53–64.